

Accretion around black holes: The geometry and spectra

B.F. Liu^{a,b,*}, Erlin Qiao^{a,b}

^a*Key Laboratory of Space Astronomy and Technology, National Astronomical
Observatories, Chinese Academy of Sciences, Beijing 100012, China*

^b*School of Astronomy and Space Sciences, University of Chinese Academy of Sciences, 19A
Yuquan Road, Beijing 100049, China*

Abstract

Observations of black hole X-ray binaries and active galactic nuclei indicate that the accretion flows around black holes are composed of hot and cold gas, which have been theoretically described in terms of either a hot geometrically thick corona lying above and below a cold geometrically thin disk or an inner advection dominated accretion flow connected to an outer thin disk. This article reviews the accretion flows around black holes, with an emphasis on the physics that determines the configuration of hot and cold accreting gas, and how the configuration varies with the accretion rate and thereby produces various luminosity and spectra.

Keywords: accretion, accretion disks, black hole physics, galaxies: active, X-rays: binaries, X-rays: galaxies

1. Introduction: solutions of accretion flow

It has been widely accepted that gas accretion onto black holes provides the principal power of radiations from black hole X-ray binaries (BHXRBS) and active galactic nuclei (AGNs). With the action of viscosity, gas captured by the black hole spirals toward the central black hole, drops off its initial angular momentum outwards, releases gravitational potential energy into heat. A frac-

*Corresponding author

Email addresses: bfliu@nao.cas.cn (B.F. Liu), qiaoel@nao.cas.cn (Erlin Qiao)

tion or all of the viscous heat is radiated, yielding a spectrum in dependence on specific radiation processes. The accretion flows are described by four basic solutions, that is, the standard thin disk (e.g. Shakura and Sunyaev, 1973), the optically thin two-temperature disk (Shapiro et al., 1976), the slim disk (e.g. Katz, 1977; Begelman, 1978; Abramowicz et al., 1988) and the advection-dominated accretion flow (e.g. Ichimaru, 1977; Rees et al., 1982; Narayan and Yi, 1994, 1995a,b; Abramowicz et al., 1995, 1996). When these solutions are applied to black holes, a composite of them are commonly adopted.

The most famous solution is the standard thin disk model developed in 1970s by Shakura and Sunyaev (1973), Novikov and Thorne (1973), Lynden-Bell and Pringle (1974)(for textbooks see Frank et al., 2002; Kato et al., 2008). The thin disk is a geometrically thin, optically thick accretion flow, characterized by multi-color blackbody radiation with effective temperatures ranging from 10^5K to 10^7K from supermassive black holes to stellar-mass black holes. The thin disk model has been the common paradigm in accretion theory and successfully used to model a large number of astrophysical systems. The most successful applications are the steady state and time-dependent nature of thin disk in dwarf novae and soft X-ray transients.

The second solution was presented by Shapiro et al. (1976), in which the accreting gas is optically thin, hot plasma with temperature near virial in ions and $\sim 10^9\text{K}$ in electrons. Such a solution is, however, thermal unstable (Piran, 1978), and is therefore not considered as applicable to black holes.

In the above two solutions, the energy released by viscous heating is assumed to be emitted locally. In contrast, a third solution was proposed (Ichimaru, 1977; Rees et al., 1982; Narayan and Yi, 1994) and extensively investigated (e.g. Narayan and Yi, 1995a,b; Abramowicz et al., 1995) (see the review Yuan and Narayan, 2014) by taking into account the advection of viscous heating. In this solution, the accreting gas has a very low density and the Coulomb coupling between the ions and electrons is weak. The viscous energy can not be radiated efficiently, instead, part of it is stored in the gas as thermal energy and eventually advected onto the black hole. Therefore, the gas forms an optically thin,

two-temperature accretion flow with the ion temperature close to virial temperature and electron temperature $T_e \sim 10^9\text{K}$, referred to as advection dominated accretion flow (ADAF). Apparently, the ADAF solution is only valid at low accretion rates so that the advection plays an important role in "digesting" the viscous heating. The radiation is, therefore, inefficient, however, contributing to hard X-ray by synchrotron self-Compton process.

The fourth solution is developed for the high accretion rate, in which the gas density is very large (e.g. Katz, 1977; Begelman, 1978; Abramowicz et al., 1988; Honma, 1996; Chen and Taam, 1993). While the viscous heating is efficiently transferred to emissions locally, most of photons are trapped in the disk, not able to escape from the disk surface during the accretion time. The energy is largely advected into the black hole in the form of photons rather than thermal energy in the ADAF solution. Therefore, the energy conversion into radiation is inefficient too. The temperature in this solution is higher than that in a standard thin disk as a result of larger accretion rate, while it is lower than that in an ADAF since ions can easily transfer viscous heat to electrons through Coulomb collisions. The disk is radiation-pressure supported, thereby the vertical scale height is larger than a standard disk, but not so extensive as an ADAF. The solution is, thus, called slim disk, sometimes referred to as an optically thick, advection-dominated accretion flow.

Other solutions of the accretion flows, the adiabatic inflow-outflow solution (ADIOS), convection-dominated accretion flow (CDAF), and the luminous hot accretion flow (LHAF) are the variants of ADAF, emphasizing the roles of outflows, convection and radiation efficiency, respectively. The ADIOS, CDAF, and LHAF are not discussed as particular solutions in addition to the ADAF.

Application of the four accretion models to black holes is constrained by both the theoretical assumption of specific models and observational luminosity and spectrum. The thin disk model applies for objects with luminosity below the Eddington luminosity, $L_{\text{Edd}} = \frac{4\pi GMm_p c}{\sigma_T}$, the critical luminosity for the outward radiation force (through Thomson scatterings) to balance the central gravity. For objects with high luminosity, slim disk model is often adopted.

Examples are the ultra-luminous X-ray sources (ULXs), the narrow-line Seyfert 1 galaxies (NLS1s), and the tidal disruption events. On the other hand, the ADAF model, characterized by its inefficient radiation and high temperature, successfully applies to the quiescent and low state BHXRBs, the Galactic center black hole, Sgr A*, and the low-luminosity AGNs.

The luminosity L is translated to the accretion rate \dot{M} with $\dot{M} = L/\eta c^2$, where η is the radiation efficiency. Accordingly, the Eddington ratio L/L_{Edd} is related to the Eddington scaled accretion rate \dot{m} , $L/L_{\text{Edd}} = (\eta/0.1)\dot{m}$, with $\dot{m} \equiv \dot{M}/\dot{M}_{\text{Edd}}$ and $\dot{M}_{\text{Edd}} \equiv L_{\text{Edd}}/0.1c^2$. By this definition, the thin disk model applies for $\dot{m} \leq 0.3$. For higher accretion rates, $\dot{m} > 0.3$, the accretion is via a slim disk, while for lower accretion rates, $\dot{m} < (0.1 - 0.3)\alpha^2$ (e.g. Narayan and Yi, 1995b; Yuan and Narayan, 2014), the accretion is via an ADAF according to the "strong ADAF principle" (Narayan and Yi, 1995b), though the thin disk is valid in this regime.

2. Theory confronted with observation: configuration of accretion flows around black holes

Black hole X-ray transient binaries can be used as a probe of the accretion process over a wide range in luminosity. The X-ray spectral behavior of these systems exhibits different states and transitions, in particular, the X-ray spectral state transition between the well-known high/soft state and low/hard state (see the reviews Tanaka and Shibazaki, 1996; Remillard and McClintock, 2006). Combined with the optical/UV observations, the X-ray observations reveal that these two spectral states originate from different accretion modes. At low luminosities the systems are characterized by a power law spectrum in hard X-rays, accompanied with a weak thermal optical component. The X-ray emission is commonly thought to be produced by the Compton scattering of soft photons off the hot electrons in an inner ADAF and the optical component by an outer truncated thin disk (e.g. Lasota et al., 1996; Dubus et al., 2001; Poutanen et al., 2018). At high luminosities the systems are characterized by a multicolor black-

body component that dominates at about 1 keV, accompanied with a weak hard tail sometimes. This has been interpreted as arising from a geometrically thin, optically thick accretion disk, covered by a weak, hot corona (e.g. Poutanen and Coppi, 1998; Gierliński et al., 1999). The transition occurs at an Eddington ratio around ~ 0.02 (e.g. Maccarone, 2003; Gierliński and Newton, 2006), though there is large difference between individual sources.

Broadband spectral features of AGNs also provide strong evidence for hot gas coexist with the thin disk in the neighborhood of the supermassive black holes (e.g. Mushotzky et al., 1993; Zdziarski et al., 1999). The big blue bump and the power-law X-ray radiation are commonly thought to be the disk thermal emission and inverse Compton scattering of the disk photons with the high-temperature electrons in the hot corona, respectively (e.g. Yuan et al., 2010). The fluorescent iron lines are explained by reflection of the corona radiation by the underlying disk (e.g. Fabian et al., 2000; Reeves et al., 2001), supporting the cold disk and hot corona scenario.

Observational data of black holes in recent years display more complicated spectral features, indicating a combination of various accretion flows (e.g. You et al., 2021; Kara et al., 2019; Ruan et al., 2019; Jin et al., 2017a,b), accompanied by wind/outflows in some cases (for observational and theoretical studies of the wind see e.g. Tombesi et al., 2010; Gofford et al., 2015; Zhu and Stone, 2018; Nomura et al., 2016; Yang et al., 2018, 2019; Wang et al., 2013; Shi et al., 2021; Yuan et al., 2015; Bu et al., 2016; Bu and Gan, 2018). A common feature of the accretion geometry in all these observations is the co-existence of hot and cool accretion flows, of which the well-known composites are either an inner ADAF connecting to a truncated disk, or an accreting corona lying above a standard thin disk which extends inward to the innermost stable circular orbit (ISCO). The former configuration was proposed by Esin et al. (1997) and applied to both quiescent BHXRBs and low-luminosity AGNs, and the latter configuration was proposed to explain the power-law X-ray emission and lower frequency blackbody component observed in both BHXRBs and AGNs (Bisnovatyi-Kogan and Blinnikov, 1976; Liang and Price, 1977; Haardt and Maraschi, 1991, 1993;

Nakamura and Osaki, 1993; Svensson and Zdziarski, 1994; Zdziarski et al., 1999).

The physical mechanism triggering the transition between such configurations has been studied since different accretion solutions were found. The “strong ADAF principle” suggests that, whenever the accreting gas has a choice between a standard thin disk and an ADAF, the ADAF configuration is chosen (Narayan and Yi, 1995b). With the radius-dependent critical accretion rate for existence of the ADAF, this rule provides a transition radius for a given accretion rate (e.g. Esin et al., 1997). In a different approach Honma (1996) determines the truncation radius by considering radial diffusive transport of heat between the inner hot accretion flows and the outer cool disk. The thermal instability in the radiation pressure-supported disk can also trigger a transition from a thin disk to an ADAF in the inner region (Gu and Lu, 2000; Lu et al., 2004). Among various possibilities, the disk and corona interaction model provides a promising explanation for the disk truncation and the spectral state transition (Liu et al., 1999; Meyer et al., 2000b,a; Różańska and Czerny, 2000; Różańska and Czerny, 2000; Meyer-Hofmeister and Meyer, 2001; Meyer and Meyer-Hofmeister, 2002; Liu et al., 2002; Spruit and Deufel, 2002; Meyer-Hofmeister and Meyer, 2003; Liu et al., 2003; Dullemond and Spruit, 2005; Liu et al., 2005, 2006, 2007; Meyer et al., 2007; Taam et al., 2008; Meyer-Hofmeister et al., 2009; Liu and Taam, 2009; Liu et al., 2011, 2012; Qiao and Liu, 2012; Taam et al., 2012; Qiao and Liu, 2013; Qiao et al., 2013; Liu and Taam, 2013; Liu, 2013; Liu et al., 2015, 2016, 2017; Meyer-Hofmeister et al., 2017; Qiao and Liu, 2017, 2018; Taam et al., 2018; Cheng et al., 2020). Specifically, the interaction between the disk and corona causes disk gas evaporating to the corona or coronal gas condensing to the disk, depending on the gas supply rate and how the gas feeds to the accretion. In the case that the accreting gas is supplied to the thin disk, as in low-mass X-ray binaries of black hole systems (LMXBs), gas evaporates from the disk to the corona. Thus, the disk is truncated when the gas supply is insufficient for evaporation. However, it extends to the ISCO when the gas supply is more than the evaporation (e.g. Meyer et al., 2000b,a; Liu et al., 2002)). In the case that the accreting gas is hot, as the wind in high-mass X-ray binaries

of black hole systems (HMXBs) or Bondi flows in AGNs, the hot accretion flow condenses partially to the disk if the supply rate is high, while it keeps the pure ADAF form if the gas supply rate is low (e.g. Liu et al., 2015; Qiao and Liu, 2018; Taam et al., 2018).

The coexistence of different accretion flows has been found by magnetohydrodynamic (MHD) simulations (e.g. Miller and Stone, 2000; Hawley and Krolik, 2001; McKinney et al., 2014; Ohsuga et al., 2005; Sadowski and Narayan, 2016). In particular, the two-phase accretion flow, either in a form of a corona overlapping a thin disk or an inner corona connecting outer thin disk, has been confirmed by the global radiation MHD simulations (e.g. Jiang et al., 2019, and references therein).

It is now widely accepted that the accretion flows around black holes are composed of hot and cold flows. The relative strength of the two flows, either the disk and the corona at high states, or the inner ADAF and the outer disk at low states is constrained by observational spectral energy distribution (SED). For instance, in modeling the soft and hard components in BHXRBS, a proper value of the truncated radius is adopted (e.g. Poutanen et al., 2018, and references therein); While in interpreting the strong X-ray emission in luminous AGN, a certain fraction of accretion energy is assumed to release in the corona (e.g. Haardt and Maraschi, 1991, 1993). Then, what is the physical mechanism that drives the formation of the hot and cold flows? How does the relative strength change? Can one determine the truncation radius consistently with observations? We'll give a detailed review aiming to answer such questions.

In the following sections, we describe the interaction between the hot and cold flows, elucidate how the interaction leads to disk truncation and consequently determines the relative strength of hot and cold accretion flows as a function of black hole mass, accretion rate and viscosity parameter, thereby producing spectra comparable with observations. Specifically, the disk evaporation model applicable to the accretion of Roche-lobe overflow (RLOF) is presented in Sect.3.1, and the corona condensation model applicable for accretion of wind is presented in Sect.3.2. The geometry of two-phase accretion flows as

a consequence of disk-corona interaction is displayed in Sect.3.3 . The radiative properties of the disk-corona system are shown and compared with observations in Sect.3.4. The conclusions are in Sect.4.

3. Formation of two-phase accretion flows around black holes

The two-phase accretion flows refer to the coexistent cold and hot accretion flows, which are, respectively, the standard thin disk and the ADAF/corona. The corona is physically similar to the ADAF excepted that a thin disk is sandwiched in. Thus, the properties of the corona, such as temperature and the optical depth, can be strongly affected by the cold thin disk via heat conduction, radiation coupling and the consequent mass exchange at a dynamic equilibrium between the disk and the corona.

The concept of the evaporation of matter from an accretion disk was originally proposed in the pioneering work by Meyer and Meyer-Hofmeister (1994) to explain the UV lag observed in dwarf novae. The model was developed in a more detailed form for application to accretion flows surrounding black holes (Liu et al., 1999; Meyer et al., 2000b,a; Meyer-Hofmeister and Meyer, 2001; Liu et al., 2002), which demonstrated the possible truncation of an outer optically thick disk and the consequent formation of an inner optically thin ADAF. The incorporation of various elements was included and the effects were investigated (Meyer and Meyer-Hofmeister, 2002; Liu et al., 2002; Meyer-Hofmeister and Meyer, 2003; Liu et al., 2005; Meyer-Hofmeister et al., 2005; Meyer-Hofmeister and Meyer, 2006; Qian et al., 2007; Qiao and Liu, 2009). Similar conceptual models, but with differences in detail were proposed in a semi-analytical model proposed (Dullemond and Spruit, 2005) and in a vertically stratified model (Różańska and Czerny, 2000; Różańska and Czerny, 2000). The coronal condensation, instead of disk evaporation, was found in the innermost region at intermediate accretion rates, leading to a weak inner disk at intermediate state (Liu et al., 2006, 2007; Meyer et al., 2007; Taam et al., 2008; Meyer-Hofmeister et al., 2009; Liu et al., 2011; Meyer-Hofmeister and Meyer, 2011; Meyer-Hofmeister

et al., 2012). The radiation spectra from such interacting disk and corona were calculated and compared with observations in BHXRBS (e.g. Qiao and Liu, 2012, 2013; Meyer-Hofmeister and Meyer, 2014; Qiao and Liu, 2015) and AGNs (e.g. Liu and Taam, 2009; Liu et al., 2012; Taam et al., 2012; Qiao et al., 2013; Liu and Taam, 2013; Liu, 2013). The condensation model was extended to the case of wind accretion and applied to HMXBs and AGN (Liu et al., 2015, 2017; Meyer-Hofmeister et al., 2017; Qiao and Liu, 2017, 2018; Taam et al., 2018; Qiao and Liu, 2019, 2020; Meyer-Hofmeister et al., 2020).

3.1. The disk evaporation model

As occurs in LMXBs, the accretion is assumed to take place via a cold thin disk as gas transferred from the donor star is constrained to the orbital plane. A corona forms above the thin disk either by processes similar to those operating in the surface of the sun, or by a thermal instability in the uppermost layers of the disk (e.g. Shaviv and Wehrse, 1986). The disk and corona are individually powered by the release of gravitational energy associated with the accretion of matter, and the interaction between the disk and corona is an important and distinctive process. Specifically, the corona is an ADAF-like accretion flow modified by the vertical heat conduction and inverse Compton scattering of disk photons, which play a key role in cooling the electrons as a consequence of the existence of an underlying disk. The ions in the corona are directly heated by viscous dissipation, partially transferring their energy to the electrons by means of Coulomb collisions. The energy gained by electrons can be effectively conducted to the lower, cooler, and denser layers by electron-electron collisions. In the lower, transition layer, the conductive heat flux is radiated away through bremsstrahlung only if the number density in this layer reaches a critical value. If the density is too low to efficiently radiate the energy, a certain amount of lower, cooler gas is heated up so that an energy equilibrium is established between the conduction, radiation and heating of the cool gas. The transfer of gas from the disk to the corona, to establish the equilibrium, is called evaporation. These processes are schematically described in Figure 1. An opposite process

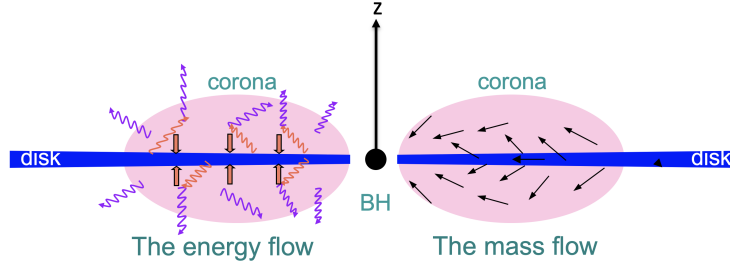


Figure 1: Schematic description of the interaction between the disk and the corona. The left part shows the vertical conduction, the direct and Compton radiations in the corona and the right part shows the gas flows.

could also take place, that is, if the density in the transition layer is too high, a certain amount of gas is over-cooled by radiation, and condenses to the disk (which is described in next subsection). The gas evaporating into the corona retains angular momentum and differentially rotates around the black hole. By frictional stresses, the gas loses angular momentum and drifts inward in such a way that the corona continuously drains gas towards the black hole. The coronal accretion flow is re-supplied by continuous evaporation and, therefore, steady flows are established in the disk and corona with the mass exchange between the two flows. The coronal accretion is supplied by evaporating disk matter. Thus, the accretion rate in the corona at a given distance is the sum of the mass evaporation from the outer disk inward to the given distance, hence it increases toward the black hole as a result of accumulation of the mass evaporation. When the accretion rate in the corona reaches a critical value, Coulomb coupling between electrons and ions is efficient so that radiation in the corona is efficient. The increased radiative cooling and decreased conductive heating to the transition layer reduce the evaporation, thereby evaporation ceases at some radius and condensation takes place in the inner region. Therefore, there exist a most efficient evaporation region where the evaporation rate reaches a maximum. If the gas supply rate to the disk is too low to replenish the disk for the evaporation, the corresponding disk region will be completely evaporated

and filled by hot gas, that is, the disk is truncated.

The corona temperature, density and mass flowing rate supplied by the evaporation can be determined by solving the equations describing the dynamics of the corona (e.g. Meyer et al., 2000b; Liu et al., 2002; Meyer-Hofmeister and Meyer, 2003; Qian et al., 2007; Qiao and Liu, 2009), as listed below.

Equation of state

$$P = \frac{\Re\rho}{2\mu}(T_i + T_e). \quad (1)$$

Equation of continuity

$$\frac{d}{dz}(\rho v_z) = \frac{2}{R}\rho v_R - \frac{2z}{R^2 + z^2}\rho v_z, \quad (2)$$

where $2z/(R^2 + z^2)$ describes the gradual expansion of the vertical flow channel with height as the geometry changes from cylindrical to spherical.

Equation of the z -component of momentum

$$\rho v_z \frac{dv_z}{dz} = -\frac{dP}{dz} - \rho \frac{GMz}{(R^2 + z^2)^{3/2}}. \quad (3)$$

The energy equation of the ions

$$\begin{aligned} & \frac{d}{dz} \left\{ \rho_i v_z \left[\frac{v^2}{2} + \frac{\gamma}{\gamma-1} \frac{P_i}{\rho_i} - \frac{GM}{(R^2+z^2)^{\frac{1}{2}}} \right] \right\} \\ &= \frac{3}{2} \alpha P \Omega - q_{ie} \\ &+ \frac{2}{R} \rho_i v_R \left[\frac{v^2}{2} + \frac{\gamma}{\gamma-1} \frac{P_i}{\rho_i} - \frac{GM}{(R^2+z^2)^{\frac{1}{2}}} \right] \\ &- \frac{2z}{R^2+z^2} \left\{ \rho_i v_z \left[\frac{v^2}{2} + \frac{\gamma}{\gamma-1} \frac{P_i}{\rho_i} - \frac{GM}{(R^2+z^2)^{\frac{1}{2}}} \right] \right\}, \end{aligned} \quad (4)$$

where q_{ie} is the energy exchange rate between the electrons and the ions through Coulomb collisions (Stepney, 1983; Liu et al., 2002),

$$q_{ie} = \left(\frac{2}{\pi} \right)^{\frac{1}{2}} \frac{3}{2} \frac{m_e}{m_p} \ln \Lambda \sigma_T c n_e n_i (\kappa T_i - \kappa T_e) \frac{1 + T_*^{\frac{1}{2}}}{T_*^{\frac{3}{2}}} \quad (5)$$

with

$$T_* = \frac{\kappa T_e}{m_e c^2} \left(1 + \frac{m_e}{m_p} \frac{T_i}{T_e} \right). \quad (6)$$

The energy equation for both the ions and the electrons is

$$\begin{aligned}
& \frac{d}{dz} \left\{ \rho v_z \left[\frac{v^2}{2} + \frac{\gamma}{\gamma-1} \frac{P}{\rho} - \frac{GM}{(R^2+z^2)^{1/2}} \right] + F_c \right\} \\
&= \frac{3}{2} \alpha P \Omega - n_e n_i L(T_e) - q_{\text{Comp}} \\
&+ \frac{2}{R} \rho v_R \left[\frac{v^2}{2} + \frac{\gamma}{\gamma-1} \frac{P}{\rho} - \frac{GM}{(R^2+z^2)^{1/2}} \right] \\
&- \frac{2z}{R^2+z^2} \left\{ \rho v_z \left[\frac{v^2}{2} + \frac{\gamma}{\gamma-1} \frac{P}{\rho} - \frac{GM}{(R^2+z^2)^{1/2}} \right] + F_c \right\},
\end{aligned} \tag{7}$$

where $n_e n_i L(T_e)$ is the bremsstrahlung cooling rate, of which the radiative cooling function $L(T_e)$ is taken from (Raymond et al., 1976); q_{Comp} is the cooling rate through inverse Compton scattering (Liu et al., 2002),

$$q_{\text{Comp}} = \frac{4\kappa T_e}{m_e c^2} n_e \sigma_T c u, \tag{8}$$

with u the energy density of the disk radiation; F_c is the thermal conduction flux given by Spitzer (1962)

$$F_c = -\kappa_0 T_e^{5/2} \frac{dT_e}{dz} \tag{9}$$

with $\kappa_0 = 10^{-6} \text{erg s}^{-1} \text{cm}^{-1} \text{K}^{-7/2}$ for a fully ionized plasma.

In the above equations, parameters M , P , ρ , T_i and T_e are the mass of black hole, the pressure, density, ion temperature and electron temperature; n_i and n_e are the number density of ions and electrons; v_z and v_R are the vertical and radial speed of the coronal flow; $\mu = 0.62$ is the mean molecular weight assuming a standard chemical composition (mass fractions of hydrogen and helium are $X = 0.75, Y = 0.25$) for the corona. Constants G , m_p and m_e are respectively is the gravitational constant, the mass of the proton and the electron; κ is the Boltzmann constant, \Re the gas constant, c the speed of light, σ Stefan-Boltzmann constant, σ_T the Thomson scattering cross section, $\gamma = 5/3$ is the ratio of specific heats, and $\ln \Lambda = 20$ is the Coulomb logarithm.

The five differential equations, Eqs.(2), (3), (4), (7), and (9), which contain five variables $P(z)$, $T_i(z)$, $T_e(z)$, $F_c(z)$, and $\dot{m}_z (\equiv \rho(z)v_z)$, can be solved with five boundary conditions. At the upper boundary, there is no artificial confinement and hence no pressure, which means a sonic transition at some height $z = H$. As there is no heat flux from/to the boundary, the upper boundary

conditions are,

$$F_c = 0 \text{ and } v_z^2 = V_s^2 \equiv P/\rho = \frac{\Re}{2\mu}(T_i + T_e) \text{ at } z = H. \quad (10)$$

At the lower boundary of the interface between the disk and corona, the conductive flux is exactly radiated away and there is no downward heat flux. The temperature of the gas should be the effective temperature of the accretion disk. Detailed investigations (Liu et al., 1995) show that the temperature increases from the effective temperature to $10^{6.5}\text{K}$ in a very thin layer and that the conductive flux can be expressed as a function of pressure at this temperature. Thus, the lower boundary conditions is reasonably approximated as (Meyer et al., 2000b)

$$T_i = T_e = 10^{6.5}\text{K}, \text{ and } F_c = -2.73 \times 10^6 P \text{ at } z = z_0. \quad (11)$$

Therefore, the coronal parameter $P(z)$, $\rho(z)$, $T_i(z)$, $T_e(z)$, evaporation rate \dot{m}_z can be determined by integrating the differential equation for given mass of black hole, $m \equiv M/M_\odot$, the mass supply rate to the disk, $\dot{m} \equiv \dot{M}/\dot{M}_{\text{Edd}}$, and viscosity parameter α . Numerical calculations of the coronal vertical structure revealed that the corona can be approximately divided into two layers, the very thin transition layer with steep variation in temperature and density along z , and the geometrically thick, hot corona with decoupled ion and electron temperature. This justifies the configuration of accretion flows as dominated by a cold disk and a hot corona connected by a very thin transition layer.

3.2. The corona condensation model

The evaporation occurs when the corona is a tenuous flow. If the density is sufficiently high so that the radiative cooling in the transition layer is more efficient than the conductive heating, a certain amount of gas is over-cooled and condenses onto the disk until energy equilibrium is reached. Efficient cooling processes in a high-density corona, such as strong inverse Compton scattering of the disk photons, can also facilitate such condensation. In the low-mass black hole X-ray binaries, condensation is weak and only occurs in the innermost

region since the corona density built up by evaporation can not be very large. In the high mass black hole X-ray binaries, wind captured by the black hole can form a strong corona and condenses to the disk on the way of accretion to the black holes. Such condensation can also occur in AGN accretion flows, accompanied by strong X-ray emission from the efficient comptonization process.

For convenient to model the radiation spectrum, the vertical structure of the disk and corona is simplified to three layers, i.e., the thin disk, the transition layer, and the corona. The parameters in the corona, such as T_i , T_e , ρ , can be determined similar to that of an ADAF, except that heat conduction and Compton scattering of disk photons are added to the energy balance equation for electrons. Thus, the disk radiation is involved in the corona equations, which depends on the accretion rate in the disk (and coronal radiation if illumination is included). Thus, given the gas supply rate in the outer boundary, the mass condensation rate can be derived as the coronal temperatures and density from the energy balance in the transition layer. This re-allocates the mass accretion rates in the disk and the corona, and in turn, affects the coronal temperatures and density. The complete set of equations is list as below.

The density and pressure in the corona are,

$$\begin{aligned}\rho &= 3.79 \times 10^{-5} \alpha^{-1} c_1^{-1} c_3^{-1/2} m^{-1} \dot{m}_c r^{-3/2} \text{ g cm}^{-3}, \\ n_e &= 2.00 \times 10^{19} \alpha^{-1} c_1^{-1} c_3^{-1/2} m^{-1} \dot{m}_c r^{-3/2} \text{ cm}^{-3}, \\ p &= 1.71 \times 10^{16} \alpha^{-1} c_1^{-1} c_3^{1/2} m^{-1} \dot{m}_c r^{-5/2} \text{ g cm}^{-1} \text{ s}^{-2},\end{aligned}\tag{12}$$

where \dot{m}_c denotes the Eddington-scaled accretion rate in the corona, m is the black hole mass in units of solar mass, r is the radius in units of Schwarzschild radius. $c_1 \approx 0.6$ and $c_3 \approx 0.4$ are insensitive to the chosen parameters (precisely, $c_1 = \frac{5+2\epsilon'}{3\alpha^2} g(\alpha, \epsilon')$, $\epsilon' = \frac{1}{f} \frac{5/3-\gamma}{\gamma-1}$, $\gamma = \frac{8-3\beta}{6-3\beta}$, $g(\alpha, \epsilon') = \left[1 + \frac{18\alpha^2}{(5+2\epsilon')^2}\right]^{1/2} - 1$, and $c_3 = (2/3)c_1$. f is the fraction of viscously dissipated energy which is advected, β is the ratio of gas pressure and total pressure).

The temperatures are determined by the self-similar solution of the sound speed ($\frac{p}{\rho} = c_s^2 = c_3 \Omega_K^2 R^2$, see Narayan and Yi (1995b))

$$T_i + 1.08T_e = 6.66 \times 10^{12} \beta c_3 r^{-1} \text{K}\tag{13}$$

and the energy balance in electrons

$$q_{ie}(\rho, T_i, T_e) = q_{\text{rad}}(\rho, T_e) + \Delta F_c/H, \quad (14)$$

where q_{ie} is the heating rate to electrons (see Eq.5), $\Delta F_c/H \approx k_0 T_e^{7/2}/H^2$ is an approximation of the conductive cooling rate, q_{rad} is the radiative cooling rate including the bremsstrahlung, synchrotron, self-Compton scattering and external Compton scattering (see Eq.8), which are the functions of T_e , ρ , and H (e.g. Narayan and Yi, 1995b; Manmoto et al., 1997) and the disk emission.

The disk is heated up by the viscous stress in the accretion and illumination from the corona, producing radiation with an effective temperature (Liu et al., 2011), $T_{\text{eff}}(R)$,

$$\sigma T_{\text{eff}}^4(R) = \frac{3GM\dot{M}_d(R)}{8\pi R^3} \left[1 - \left(\frac{3R_S}{R} \right)^{1/2} \right] + \frac{(1-a)L_{\text{c,int}}}{8\pi} \frac{H_s}{(R^2 + H_s^2)^{3/2}} \quad (15)$$

where $\dot{M}_d(R)$ denotes the accretion rate in the disk, $L_{\text{c,int}} = 2 \int q_{\text{rad}} 2\pi R H dR$ is volume-integrated radiation luminosity from the corona on both sides of the disk, $H_s \sim (3-10)R_s$ is the height of the coronal illumination approximated as a lamppost, and a is albedo of the disk. Therefore, the soft photon involved in the inverse Compton scattering in the corona is dominated by the local disk radiation in the inner region with an energy density $u = (2/c)\sigma T_{\text{eff}}^4$; While in the outer region, photons emitted from the inner disk could overwhelm the local disk emission. Thus, the energy density $u(R)$ for Compton scattering can be approximated by

$$u(R) \approx \frac{2}{c} \max \left[\sigma T_{\text{eff}}^4(R), (1 - 1/\sqrt{2}) \frac{L_d}{8\pi R^2} \right], \quad (16)$$

where the second term represents vertically averaged irradiation of disk emission to the outer corona (L_d the total disk luminosity) (Liu et al., 2003).

From Eqs.(12), (13),(14), (16) the temperatures (T_i , T_e) and the density (ρ or n_e) in the corona, and the effective temperature in the disk can be calculated numerically for given α , β , a , m , R , provided that the accretion rate in the corona (\dot{m}_c), and in the disk (\dot{M}_d) are known.

Given the corona temperature and density, the evaporation rate at unit surface area can be derived from the transition layer, that is (e.g. Liu et al., 2007; Meyer et al., 2007),

$$\dot{m}_z = \frac{\gamma - 1}{\gamma} \beta \frac{-F_c}{kT_i/\mu_i m_p} (1 - \sqrt{C}) \quad (17)$$

with

$$C = \kappa_0 b \left(\frac{\beta^2 p^2}{\pi k^2} \right) \left(\frac{T_{\text{cpl}}}{F_c} \right)^2, \quad (18)$$

where $b = 10^{-26.56} \text{g cm}^5 \text{s}^{-3} \text{K}^{-1/2}$, $F_c \approx -k_0 T_e^{7/2}/H$, and T_{cpl} the coupling temperature in the transition layer determined by the energy balance ($q^+ + q^c = q_{\text{ie}}$ with compressive heating rate $q^c = \frac{f}{1-\beta} q^+$) in this layer. T_i and p are the ion temperature and pressure of the corona.

The positive value of \dot{m}_z means that gas evaporates from the disk to the corona, while negative \dot{m}_z means that gas condenses from the corona to the disk. As a consequence, the accretion rates in the disk and in the corona vary with the distance. The integrated evaporation/condensation rate (in unit of Eddington rate \dot{M}_{Edd}) from R to the outer boundary R_b is

$$\dot{m}_{\text{evap}}(R) = \int_R^{R_b} \frac{4\pi R}{\dot{M}_{\text{Edd}}} \dot{m}_z dR. \quad (19)$$

If the gas captured by the black hole is supplied to disk at a rate of \dot{m} , as the Roche-lobe overflow in the LMXBs, disk gas will evaporate to the corona when it accretes toward the black hole. The accretion rates at distance R via the disk and the corona are, respectively,

$$\dot{m}_{\text{d}}(R) = \dot{m} - \dot{m}_{\text{evap}}(R) \quad \text{and} \quad \dot{m}_{\text{c}}(R) = \dot{m}_{\text{evap}}(R). \quad (20)$$

If the gas is supplied to the corona at a rate of \dot{m} , gas can condense to the disk when the gas supply rate is sufficiently high. We then have

$$\dot{m}_{\text{d}}(R) = -\dot{m}_{\text{evap}}(R) \quad \text{and} \quad \dot{m}_{\text{c}}(R) = \dot{m} + \dot{m}_{\text{evap}}(R). \quad (21)$$

As the $\dot{m}_{\text{evap}}(R)$ is an implicit function of T_i , T_e , ρ , and T_{eff} for given α , β , a , m , R , \dot{m} , the accretion rates in disk and in corona are the implicit function of

T_i , T_e , ρ , and T_{eff} . Therefore, Eqs.(12), (13),(14), (15) are a complete set of equations when the accretion rates in disk and corona are expressed by Eq.(20) or Eq.(21). Solving the equations we determine the the disk and corona characteristic parameters T_i , T_e , ρ , and T_{eff} . Other quantities, such as the pressure, viscosity heating rate and its advection fraction, the evaporation/condensation rate, the radiation cooling functions by different processes, are also functions of T_i , T_e , ρ , T_{eff} and involved in calculating the characteristic parameters.

3.3. Consequence of disk-corona interaction: the two-phase accretion flows

Interaction of the disk and corona results in gas exchange between the two accretion flows, with an evaporation/condensation rate in dependence on the property of the two flows. The final steady geometry of the accretion flows depends not only on the mass-supply rate, but also on how the gas is supplied to the accretion, the RLOF or the wind.

In the case of RLOF supply to the thin disk, the coronal flow increases during its accretion toward the black hole as the evaporation gas continuously joins; Meanwhile the radiation efficiency increases, which depresses the evaporation from some distance inwards. Thus, the evaporation rate is expected to reach a maximum value and decreases in the innermost region, as shown by numerical computation. While the evaporation process diverts the accretion flow from the disk to the corona, the disk is completely evaporated within a specific region for lower gas supply rates. This region is filled with coronal gas, and the accretion takes place in a geometrically thick, hot flow. On the other hand, for gas supply rate higher than the maximal evaporation rate, the optically thick disk cannot be significantly depleted at any distance. Thus, the disk extends to the ISCO with an overlying accreting coronal flow coexisting with the disk, where continuous evaporation feeds the corona accretion. The typical accretion geometry is displayed in Figure 2.

The evolution of accretion geometry during an outburst of LMXBs is illustrated in Figure 3. On the rise of an outburst the accretion rate increases, pushing the truncated disk inwards. When the critical accretion rate (of ~ 0.02)

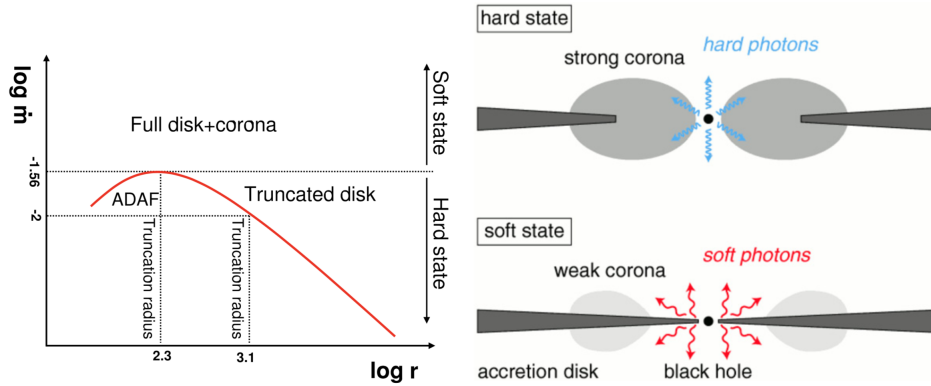


Figure 2: Schematic description of disk truncation and the spectral transition illustrating its dependence on the mass accretion rate. The evaporation rate (in units of Eddington rate) is illustrated as a function of the distance (in units of Schwarzschild radius) in the left panel. At low accretion rates supplied by RLOF, the disk is truncated by evaporation due to insufficient mass supply at distances determined by the evaporation curve, When the RLOF rate exceeds the maximum, evaporation cannot evacuate any disk region, thus, the disk extends to the ISCO and dominates the accretion flow. Figure from Liu and Taam (2009)

is reached, the thin disk extends to the ISCO. Further increase of accretion rate in the disk leads to efficient Compton cooling and hence condensation of coronal gas. Then the corona becomes very tenuous. During the decay, the disk weakens with decrease of accretion rate, is truncated at the most efficient evaporation region when the accretion rate decreases to a lower critical value, leaving an inner disk at the intermediate state; The inner disk eventually disappears with further decrease of accretion rate.

In the case of wind supply, the spatial extent and thermal state of the accretion flow in the outer regions can significantly differ from the RLOF. As revealed by the 3D hydrodynamical simulations (Walder et al., 2014), the mass captured from a stellar wind is heated at the bow shock to temperatures of $\sim 10^7\text{K}$, supplied to the accretion in a hot rather than in a cool physical state. Such gas is not necessarily constrained to lie in the disk plane, and hence can form a hot accretion flow as a consequence of inefficient radiative cooling in a

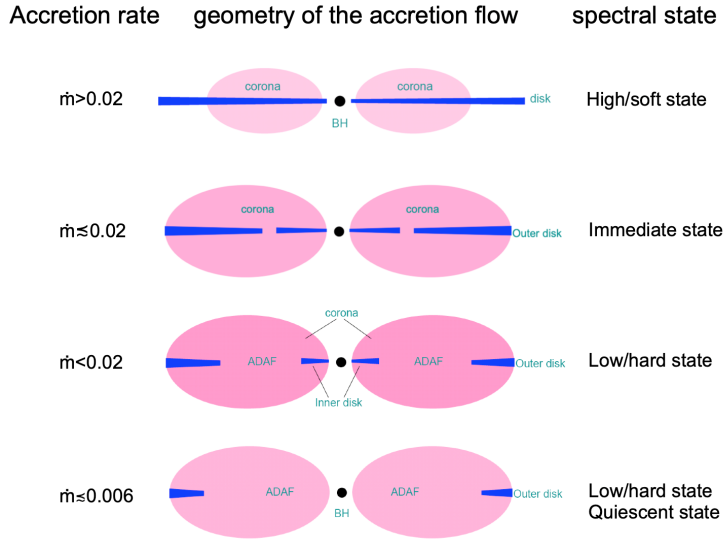


Figure 3: Variation of the accretion flow geometry and spectral states with the accretion rate of gas supplied to the thin disk, as the Roche-lobe overflow in low mass X-ray binaries. The disk truncation radius moves inwards with increase of gas supply rate as a sequence of equilibrium of evaporation and inflow of gas in the disk; When the gas supply rate is larger than the maximal evaporation rate, the disk cannot be truncated anymore, in stead, the evaporation-fed corona becomes weak as the increased Compton cooling to the corona restrains the evaporation. An inner disk occurs during the decay of an outburst since the disk is first depleted at the most efficiently evaporating region around 200 Schwarzschild radii. The inner disk becomes small with decrease of gas supply rate and eventually disappears.

geometrically thick flow, i.e., ADAF. By studying such an ADAF interacting with a pre-existing disk, it is found that the accretion geometry depends on the accretion rate supplied by the wind or interstellar medium. At low accretion rates, the gas evaporates from the thin disk, quickly evacuating the thin disk, if existing initially. Thus, the accretion is via ADAF when it reaches a steady state. This result is similar to that of cold gas supply to a thin disk, e.g. the RLOF supply. At high accretion rate, it is found that the hot gas partially condenses to the underlying cool disk as it flows toward the black hole. Such a thin accretion disk can be maintained in a steady state with gas continuously condensing to the disk. Since the condensation efficiency depends on the gas supply rate, the radial distribution of mass flow rates in the hot and cool components varies with the accretion rate supplied by winds, in particular, the thin disk can be maintained exist only in a limited radial scale in the neighborhood of the black hole. Therefore, the disk size and its strength relative to the corona depends on the wind supply rate. The variation of accretion flow geometry with wind supply rate is displayed in Figure 4.

It is displayed above that the accretion flow is a combination of hot and cold flows, dominated by the ADAF at low accretion rates, while by the thin disk at high accretion rates. Such a conclusion is valid no matter the accretion gas is supplied by RLOF or by wind/interstellar medium. This is essential as the hot gas inevitably interacts with the cold gas during the accretion. The variation of the gas supply rate changes the relative strength of the thin disk and the hot accretion flow, leading to a change in the spectrum and even state transition, as discussed in the following section.

3.4. The radiative properties as compared with observations

The emission of accretion flows comes dominantly from the inner region, as a results of release of gravitational energy into radiation. Given the fact that the radiation efficiency of hot gas increases toward the black hole (as a consequence of efficient Coulomb coupling at inner region), the corona (or ADAF) emission is even more dominated by the inner region (Liu et al., 2017), no matter the

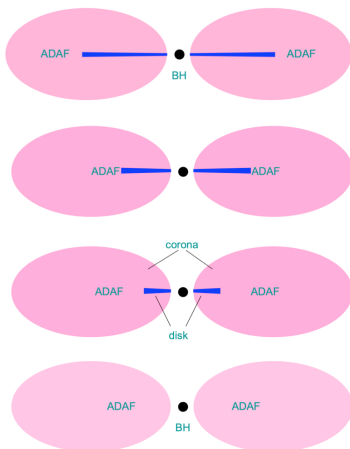


Figure 4: Variation of the accretion flow geometry with accretion rate of gas supplied by wind, as that in high mass X-ray binaries or AGNs. The weak wind captured by the black hole forms an ADAF; When the wind supply rate increases to a critical value, part of the corona gas can collapse to form a weak disk in the inner region as a result of over-cooling; Further increase of wind supply leads to strong condensation and a large disk.

corona is compact or extended. Therefore, the total radiation and SED from the disk and corona are not significantly affected by the style of gas supply, but are determined by accretion rates flowing respectively in the inner disk and inner corona, which are eventually determined by the the gas supply rate. An example of spectral variation with the gas supply rate from the accretion flows is displayed in Figure 5 for the case of wind accretion. The left panel of the figure shows that the spectra are soft at high accretion rate, with strong disk emission and steep X-ray spectrum. This is caused by the strong condensation of coronal gas to the disk. When the accretion rate decreases, condensation becomes weak, thereby the accretion rate in the disk decreases, as shown in the right panel of Figure 5. Condensation stops when the gas supply rate decreases to ~ 0.02 . Correspondingly, the spectrum undergoes transition from soft state to hard state.

We note that the relative strength of disk and corona, and hence the emission spectrum, also depend on the viscosity parameter (α), the magnetic field

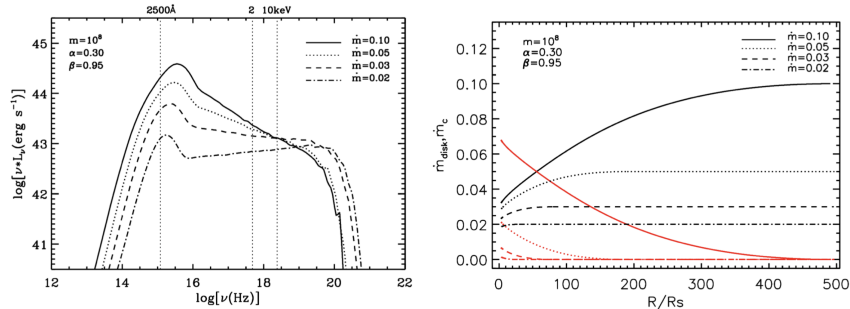


Figure 5: Mass flow rate in the disk and corona (right panel) and the corresponding spectra (left panel). Left panel: Spectra emitted from a disk and corona with a hot mass supply for a black hole of $10^8 M_\odot$, viscosity parameter $\alpha = 0.3$, magnetic field parameter $\beta = 0.95$, albedo $a = 0.15$. Curves from bottom to top refer to mass supply rates of 0.02, 0.03, 0.05, and 0.1. Right panel: The corresponding radial distribution of the mass flow rate in the disk and corona caused by condensation. Curves in red (black) refer to the mass flow rate in the disk (corona). Figure adapted from (Qiao and Liu, 2017)

(parameterized in β), and the albedo (a) of the disk (Qiao and Liu, 2018). A larger value of α means more heating, leading to a stronger corona and harder X-ray spectrum; The spectrum is not sensitive to the magnetic field if the magnetic energy is no larger than the energy of equipartition (i.e. $0.5 < \beta < 1$); The effect of albedo is also not very important since it varies only in a limit range, for example, $a = 0.1 - 0.2$ for a disk around AGN (Haardt and Maraschi, 1993). Nevertheless, a change in the combination of the three parameters can, to some extent, change the geometry of the two-phase accretion flows, thereby change the overall spectral shape. The effects of viscosity and magnetic field on the spectra for $a = 0.15$ are shown in Figure 6.

Therefore, the two-phase accretion flows can produce various types of spectra, which are mainly determined by the gas supply rates, modified by the value of viscosity as well as magnetic field and albedo. The transition of spectral states can occur at an accretion rate depending on the viscous parameter and evolution history (from hard to soft state or from soft to hard state). The model naturally interprets the diversity of spectra and state transition of black holes.

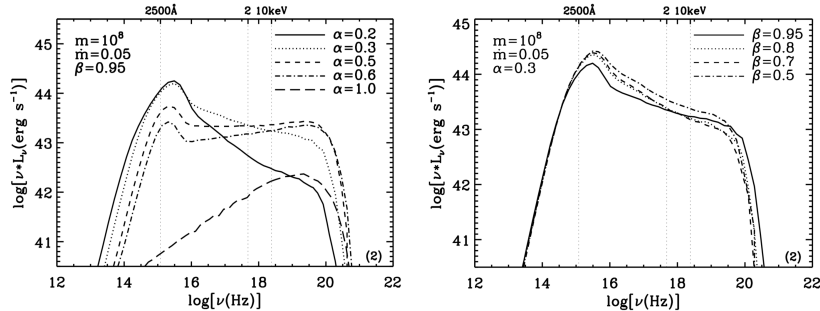


Figure 6: Spectra dependent on the viscosity (Left panel) and magnetic field (Right Panel). Figures from (Qiao and Liu, 2018)

While the general features of the stationary accretion flows are similar for the accretion supplied by RLOF and wind, there exist some differences. In contrast to the extensive thin disk formed from RLOF, the disk is much smaller as fed by the condensation of hot wind because the radiative cooling at outer region is insufficient to cause condensation. The absence of an outer disk precludes the possibility of thermal instabilities in the hydrogen ionization zone and therefore the large outbursts. This interprets why Cyg X-1 is a persistent source with no large outburst, unlike the transient sources. Luminosity fluctuations in the wind-fed sources would be a consequence of turbulence in the accretion wake region, which are likely smaller than that caused by thermal instabilities. Thus, the wind-fed sources could be described as persistent, varying occasionally between soft and hard spectral states with a relatively small amplitude.

The second difference is the presence/absence of hysteresis between the transition luminosities at hard-to-soft and soft-to-hard transitions. The hysteresis in the light curve of transient sources (e.g. Maccarone and Coppi, 2003; Zdziarski and Gierliński, 2004) is thought to be caused by the large difference in Compton cooling rate before the state transitions (Liu et al., 2005; Meyer-Hofmeister et al., 2005). When the transient sources are in a deep quiescent state before outbursts are triggered, the evaporation is efficient as there is no/weak Compton cooling in the corona. Only when the accretion rate exceeds the maximal

evaporation rate can the disk is fully filled in and spectral state transits. During the decay of an outburst the strong disk radiation involved in Compton scattering depresses the disk evaporation, which leads to the disk to be truncated at a lower accretion rate. However, this effect is insignificant in persistent sources because of a small difference in the variation of accretion rate in the hard and soft states (Taam et al., 2018). Therefore, the light curve during the transition between states is likely to be more symmetrical in persistent systems, as it is observed in Cyg X-1.

The third distinction is that the accretion rates remained in the innermost corona are similar ($\dot{m}_c \sim 0.02$) for different rates of the hot gas supply ($\dot{m} > 0.02$). This is in contrast to the conclusion from RLOF that very little gas accretes via a corona at a high gas supply rates, i.e. the higher gas supply rate, the lower rate in the corona. Therefore, the X-ray emission in wind accretion systems, which originates from the liberation of gravitational energy of the coronal gas and enthalpy of the condensed gas, can be larger than that with only cold gas supply to the disk (e.g. RLOF). Hence, the wind accretion model provides insight to the generation of strong X-ray radiation in luminous AGNs without necessarily invoking artificially heating to the corona.

Finally, there should be difference in timing properties between the accretion of RLOF and wind, if spatial region of hot and cold gas is involved in producing the noise component.

4. Conclusion

This paper reviews the physics of formation of multi-phase accretion flows around black holes. Of importance is the fact that the coupling between the cold and hot gas leads to gas evaporation or condensation, thereby the formation of various configurations of accretion flows as a function of accretion rate and system parameters. In particular, it shows how the gas supply affects the accretion configuration. For the Roche-lobe overflow supply, as in low mass X-ray binaries, evaporation from the disk leads to accretion via a thin disk sandwiched in a

corona at high accretion rates, and an inner ADAF connecting to an outer disk at low accretion rates; For the wind or interstellar medium supply, an ADAF forms and extends to ISCO at low accretion rates, while a thin disk forms in the inner region owing to hot gas condensation, which is coexisted with the left corona at high accretion rates. The different configuration caused by different gas supply does not significantly affect the radiation spectrum, except for the relatively strong coronal emission in the case of wind supply. However, it does cause different variability features, such as the presence/absence of hysteresis in transition luminosity, the transient behavior in LMXBs and persistent behavior in Cyg X-1.

Acknowledgments: Financial support for this work is provided by the National Natural Science Foundation of China (grants 12073037 and 11773037) and NAOC Nebula Talents Program.

References

- Abramowicz, M.A., Chen, X., Kato, S., Lasota, J.P., Regev, O., 1995. Thermal Equilibria of Accretion Disks. *ApJL* 438, L37. doi:10.1086/187709, arXiv:astro-ph/9409018.
- Abramowicz, M.A., Chen, X.M., Granath, M., Lasota, J.P., 1996. Advection-dominated Accretion Flows around Kerr Black Holes. *ApJ* 471, 762. doi:10.1086/178004, arXiv:astro-ph/9607021.
- Abramowicz, M.A., Czerny, B., Lasota, J.P., Szuszkiewicz, E., 1988. Slim Accretion Disks. *ApJ* 332, 646. doi:10.1086/166683.
- Begelman, M.C., 1978. Black holes in radiation-dominated gas: an analogue of the Bondi accretion problem. *MNRAS* 184, 53–67. doi:10.1093/mnras/184.1.53.
- Bisnovatyi-Kogan, G.S., Blinnikov, S.I., 1976. A hot corona around a black-hole accretion disk as a model for CYG X-1. *Soviet Astronomy Letters* 2, 191–193. arXiv:astro-ph/0003275.

- Bu, D.F., Gan, Z.M., 2018. On the wind production from hot accretion flows with different accretion rates. *MNRAS* 474, 1206–1213. doi:10.1093/mnras/stx2894, arXiv:1711.02238.
- Bu, D.F., Yuan, F., Gan, Z.M., Yang, X.H., 2016. Hydrodynamical Numerical Simulation of Wind Production from Black Hole Hot Accretion Flows at Very Large Radii. *ApJ* 818, 83. doi:10.3847/0004-637X/818/1/83, arXiv:1510.03124.
- Chen, X., Taam, R.E., 1993. The Structure and Stability of Transonic Accretion Disks Surrounding Black Holes. *ApJ* 412, 254. doi:10.1086/172916.
- Cheng, H., Liu, B.F., Liu, J., Liu, Z., Qiao, E., Yuan, W., 2020. Magnetic-reconnection-heated corona in active galactic nuclei: refined disc-corona model and application to broad-band radiation. *MNRAS* 495, 1158–1171. doi:10.1093/mnras/staa1250, arXiv:2006.02665.
- Dubus, G., Hameury, J.M., Lasota, J.P., 2001. The disc instability model for X-ray transients: Evidence for truncation and irradiation. *A&A* 373, 251–271. doi:10.1051/0004-6361:20010632, arXiv:astro-ph/0102237.
- Dullemond, C.P., Spruit, H.C., 2005. Evaporation of ion-irradiated disks. *A&A* 434, 415–422. doi:10.1051/0004-6361:20042517, arXiv:astro-ph/0501463.
- Esin, A.A., McClintock, J.E., Narayan, R., 1997. Advection-Dominated Accretion and the Spectral States of Black Hole X-Ray Binaries: Application to Nova Muscae 1991. *ApJ* 489, 865–889. doi:10.1086/304829, arXiv:astro-ph/9705237.
- Fabian, A.C., Iwasawa, K., Reynolds, C.S., Young, A.J., 2000. Broad Iron Lines in Active Galactic Nuclei. *PASP* 112, 1145–1161. doi:10.1086/316610, arXiv:astro-ph/0004366.
- Frank, J., King, A., Raine, D.J., 2002. *Accretion Power in Astrophysics: Third Edition*.

- Gierliński, M., Newton, J., 2006. X-ray spectral transitions of black holes from RXTE All-Sky Monitor. *MNRAS* 370, 837–844. doi:10.1111/j.1365-2966.2006.10514.x, arXiv:astro-ph/0601676.
- Gierliński, M., Zdziarski, A.A., Poutanen, J., Coppi, P.S., Ebisawa, K., Johnson, W.N., 1999. Radiation mechanisms and geometry of Cygnus X-1 in the soft state. *MNRAS* 309, 496–512. doi:10.1046/j.1365-8711.1999.02875.x, arXiv:astro-ph/9905146.
- Gofford, J., Reeves, J.N., McLaughlin, D.E., Braitto, V., Turner, T.J., Tombesi, F., Cappi, M., 2015. The Suzaku view of highly ionized outflows in AGN - II. Location, energetics and scalings with bolometric luminosity. *MNRAS* 451, 4169–4182. doi:10.1093/mnras/stv1207, arXiv:1506.00614.
- Gu, W.M., Lu, J.F., 2000. Bimodal Accretion Disks: Shakura-Sunyaev Disk-Advection-dominated Accretion Flow Transitions. *ApJL* 540, L33–L36. doi:10.1086/312864.
- Haardt, F., Maraschi, L., 1991. A two-phase model for the X-ray emission from Seyfert galaxies. *ApJL* 380, L51–L54. doi:10.1086/186171.
- Haardt, F., Maraschi, L., 1993. X-ray spectra from two-phase accretion disks. *ApJ* 413, 507–517. doi:10.1086/173020.
- Hawley, J.F., Krolik, J.H., 2001. Global MHD Simulation of the Inner Accretion Disk in a Pseudo-Newtonian Potential. *ApJ* 548, 348–367. doi:10.1086/318678, arXiv:astro-ph/0006456.
- Honma, F., 1996. Global Structure of Bimodal Accretion Disks around a Black Hole. *PASJ* 48, 77–87. doi:10.1093/pasj/48.1.77.
- Ichimaru, S., 1977. Bimodal behavior of accretion disks: theory and application to Cygnus X-1 transitions. *ApJ* 214, 840–855. doi:10.1086/155314.
- Jiang, Y.F., Blaes, O., Stone, J.M., Davis, S.W., 2019. Global Radiation Magnetohydrodynamic Simulations of sub-Eddington Accretion Disks around Su-

- permissive Black Holes. *ApJ* 885, 144. doi:10.3847/1538-4357/ab4a00, arXiv:1904.01674.
- Jin, C., Done, C., Ward, M., 2017a. Super-Eddington QSO RX J0439.6-5311 - I. Origin of the soft X-ray excess and structure of the inner accretion flow. *MNRAS* 468, 3663–3681. doi:10.1093/mnras/stx718, arXiv:1703.07118.
- Jin, C., Done, C., Ward, M., Gardner, E., 2017b. Super-Eddington QSO RX J0439.6-5311 - II. Multiwavelength constraints on the global structure of the accretion flow. *MNRAS* 471, 706–721. doi:10.1093/mnras/stx1634, arXiv:1706.08125.
- Kara, E., Steiner, J.F., Fabian, A.C., Cackett, E.M., Uttley, P., Remillard, R.A., Gendreau, K.C., Arzoumanian, Z., Altamirano, D., Eikenberry, S., Enoto, T., Homan, J., Neilsen, J., Stevens, A.L., 2019. The corona contracts in a black-hole transient. *Nature* 565, 198–201. doi:10.1038/s41586-018-0803-x, arXiv:1901.03877.
- Kato, S., Fukue, J., Mineshige, S., 2008. Black-Hole Accretion Disks — Towards a New Paradigm —.
- Katz, J.I., 1977. X-rays from spherical accretion onto degenerate dwarfs. *ApJ* 215, 265–275. doi:10.1086/155355.
- Lasota, J.P., Narayan, R., Yi, I., 1996. Mechanisms for the outbursts of soft X-ray transients. *A&A* 314, 813–820. arXiv:astro-ph/9605011.
- Liang, E.P.T., Price, R.H., 1977. Accretion disk coronae and Cygnus X-1. *ApJ* 218, 247–252. doi:10.1086/155677.
- Liu, B.F., 2013. Coupling of the accretion disk and corona around black holes, in: Zhang, C.M., Belloni, T., Méndez, M., Zhang, S.N. (Eds.), *Feeding Compact Objects: Accretion on All Scales*, pp. 62–65. doi:10.1017/S1743921312019217.

- Liu, B.F., Done, C., Taam, R.E., 2011. The Effect of Coronal Radiation on a Residual Inner Disk in the Low/Hard Spectral State of Black Hole X-ray Binary Systems. *ApJ* 726, 10. doi:10.1088/0004-637X/726/1/10, arXiv:1011.2580.
- Liu, B.F., Meyer, F., Meyer-Hofmeister, E., 2005. Spectral state transitions in low-mass X-ray binaries - the effect of hard and soft irradiation. *A&A* 442, 555–562. doi:10.1051/0004-6361:20053207, arXiv:astro-ph/0506444.
- Liu, B.F., Meyer, F., Meyer-Hofmeister, E., 2006. An inner disk below the ADAF: the intermediate spectral state of black hole accretion. *A&A* 454, L9–L12. doi:10.1051/0004-6361:20065430, arXiv:astro-ph/0606217.
- Liu, B.F., Mineshige, S., Meyer, F., Meyer-Hofmeister, E., Kawaguchi, T., 2002. Two-Temperature Coronal Flow above a Thin Disk. *ApJ* 575, 117–126. doi:10.1086/341138, arXiv:astro-ph/0204174.
- Liu, B.F., Mineshige, S., Ohsuga, K., 2003. Spectra from a Magnetic Reconnection-heated Corona in Active Galactic Nuclei. *ApJ* 587, 571–579. doi:10.1086/368282, arXiv:astro-ph/0301142.
- Liu, B.F., Taam, R.E., 2009. Application of the Disk Evaporation Model to Active Galactic Nuclei. *ApJ* 707, 233–242. doi:10.1088/0004-637X/707/1/233, arXiv:0910.3725.
- Liu, B.F., Taam, R.E., 2013. Constraints on the Viscosity and Magnetic Field in Hot Accretion Flows around Black Holes. *ApJS* 207, 17. doi:10.1088/0067-0049/207/1/17, arXiv:1306.5881.
- Liu, B.F., Taam, R.E., Meyer-Hofmeister, E., Meyer, F., 2007. The Existence of Inner Cool Disks in the Low/Hard State of Accreting Black Holes. *ApJ* 671, 695–705. doi:10.1086/522619, arXiv:0709.0143.
- Liu, B.F., Taam, R.E., Qiao, E., Yuan, W., 2015. A Hybrid Two Component Accretion Flow Surrounding Supermassive Black Holes in AGNs. *ApJ* 806, 223. doi:10.1088/0004-637X/806/2/223, arXiv:1505.00551.

- Liu, B.F., Taam, R.E., Qiao, E., Yuan, W., 2017. Centrally Concentrated X-Ray Radiation from an Extended Accreting Corona in Active Galactic Nuclei. *ApJ* 847, 96. doi:10.3847/1538-4357/aa894c, arXiv:1709.09799.
- Liu, B.F., Yuan, W., Meyer, F., Meyer-Hofmeister, E., Xie, G.Z., 1999. Evaporation of Accretion Disks around Black Holes: The Disk-Corona Transition and the Connection to the Advection-dominated Accretion Flow. *ApJL* 527, L17–L20. doi:10.1086/312383, arXiv:astro-ph/9911051.
- Liu, F.K., Meyer, F., Meyer-Hofmeister, E., 1995. Dwarf novae in quiescence: the relationship between disk evaporation and accretion onto a white dwarf. *A&A* 300, 823.
- Liu, J.Y., Liu, B.F., Qiao, E.L., Mineshige, S., 2012. The Structure and Spectral Features of a Thin Disk and Evaporation-fed Corona in High-luminosity Active Galactic Nuclei. *ApJ* 754, 81. doi:10.1088/0004-637X/754/2/81, arXiv:1205.6958.
- Liu, J.Y., Qiao, E.L., Liu, B.F., 2016. Revisiting the Structure and Spectrum of the Magnetic-reconnection-heated Corona in Luminous AGNs. *ApJ* 833, 35. doi:10.3847/1538-4357/833/1/35, arXiv:1611.07149.
- Lu, J.F., Lin, Y.Q., Gu, W.M., 2004. The Shakura-Sunyaev Disk Can Smoothly Match an Advection-dominated Accretion Flow. *ApJL* 602, L37–L40. doi:10.1086/382209, arXiv:astro-ph/0401018.
- Lynden-Bell, D., Pringle, J.E., 1974. The evolution of viscous discs and the origin of the nebular variables. *MNRAS* 168, 603–637. doi:10.1093/mnras/168.3.603.
- Maccarone, T.J., 2003. Do X-ray binary spectral state transition luminosities vary? *A&A* 409, 697–706. doi:10.1051/0004-6361:20031146, arXiv:astro-ph/0308036.

- Maccarone, T.J., Coppi, P.S., 2003. Hysteresis in the light curves of soft X-ray transients. *MNRAS* 338, 189–196. doi:10.1046/j.1365-8711.2003.06040.x, arXiv:astro-ph/0209116.
- Manmoto, T., Mineshige, S., Kusunose, M., 1997. Spectrum of Optically Thin Advection-dominated Accretion Flow around a Black Hole: Application to Sagittarius A*. *ApJ* 489, 791–803. doi:10.1086/304817, arXiv:astro-ph/9708234.
- McKinney, J.C., Tchekhovskoy, A., Sadowski, A., Narayan, R., 2014. Three-dimensional general relativistic radiation magnetohydrodynamical simulation of super-Eddington accretion, using a new code HARMRAD with M1 closure. *MNRAS* 441, 3177–3208. doi:10.1093/mnras/stu762, arXiv:1312.6127.
- Meyer, F., Liu, B.F., Meyer-Hofmeister, E., 2000a. Black hole X-ray binaries: a new view on soft-hard spectral transitions. *A&A* 354, L67–L70. arXiv:astro-ph/0002053.
- Meyer, F., Liu, B.F., Meyer-Hofmeister, E., 2000b. Evaporation: The change from accretion via a thin disk to a coronal flow. *A&A* 361, 175–188. arXiv:astro-ph/0007091.
- Meyer, F., Liu, B.F., Meyer-Hofmeister, E., 2007. Re-condensation from an ADAF into an inner disk: the intermediate state of black hole accretion? *A&A* 463, 1–9. doi:10.1051/0004-6361:20066203, arXiv:astro-ph/0611487.
- Meyer, F., Meyer-Hofmeister, E., 1994. Accretion disk evaporation by a coronal siphon flow. *A&A* 288, 175–182.
- Meyer, F., Meyer-Hofmeister, E., 2002. The effect of disk magnetic fields on the truncation of geometrically thin disks in AGN. *A&A* 392, L5–L8. doi:10.1051/0004-6361:20021075, arXiv:astro-ph/0207573.
- Meyer-Hofmeister, E., Liu, B.F., Meyer, F., 2005. Hysteresis in spectral state transitions - a challenge for theoretical modeling. *A&A* 432, 181–187. doi:10.1051/0004-6361:20041631, arXiv:astro-ph/0411145.

- Meyer-Hofmeister, E., Liu, B.F., Meyer, F., 2009. The hard to soft spectral transition in LMXBs-affected by recondensation of gas into an inner disk. *A&A* 508, 329–337. doi:10.1051/0004-6361/200913044, arXiv:0910.4273.
- Meyer-Hofmeister, E., Liu, B.F., Meyer, F., 2012. Coronae above accretion disks around black holes: the effect of Compton cooling. *A&A* 544, A87. doi:10.1051/0004-6361/201219245, arXiv:1208.0265.
- Meyer-Hofmeister, E., Liu, B.F., Qiao, E., 2017. Interaction of the accretion flows in corona and disk near the black hole in active galactic nuclei. *A&A* 607, A94. doi:10.1051/0004-6361/201731105, arXiv:1712.02031.
- Meyer-Hofmeister, E., Liu, B.F., Qiao, E., Taam, R.E., 2020. Wind accretion in Cygnus X-1. *A&A* 637, A66. doi:10.1051/0004-6361/202037561, arXiv:2004.13241.
- Meyer-Hofmeister, E., Meyer, F., 2001. The change from accretion via a thin disk to a coronal flow: Dependence on the viscosity of the hot gas. *A&A* 380, 739–744. doi:10.1051/0004-6361:20011449, arXiv:astro-ph/0112431.
- Meyer-Hofmeister, E., Meyer, F., 2003. The formation of the coronal flow/ADAF. *A&A* 402, 1013–1019. doi:10.1051/0004-6361:20030320, arXiv:astro-ph/0303525.
- Meyer-Hofmeister, E., Meyer, F., 2006. The effect of heat conduction on the interaction of disk and corona around black holes. *A&A* 449, 443–447. doi:10.1051/0004-6361:20053997, arXiv:astro-ph/0512528.
- Meyer-Hofmeister, E., Meyer, F., 2011. Broad iron emission lines in Seyfert galaxies - re-condensation of gas onto an inner disk below the ADAF? *A&A* 527, A127. doi:10.1051/0004-6361/201015478, arXiv:1101.4854.
- Meyer-Hofmeister, E., Meyer, F., 2014. The relation between radio and X-ray luminosity of black hole binaries: affected by inner cool disks? *A&A* 562, A142. doi:10.1051/0004-6361/201322423, arXiv:1401.7525.

- Miller, K.A., Stone, J.M., 2000. The Formation and Structure of a Strongly Magnetized Corona above a Weakly Magnetized Accretion Disk. *ApJ* 534, 398–419. doi:10.1086/308736, arXiv:astro-ph/9912135.
- Mushotzky, R.F., Done, C., Pounds, K.A., 1993. X-ray spectra and time variability of active galactic nuclei. *ARA&A* 31, 717–717. doi:10.1146/annurev.aa.31.090193.003441.
- Nakamura, K., Osaki, Y., 1993. Self-consistent accretion disk-coronal model for active galactic nuclei. *PASJ* 45, 775–787.
- Narayan, R., Yi, I., 1994. Advection-dominated Accretion: A Self-similar Solution. *ApJL* 428, L13. doi:10.1086/187381, arXiv:astro-ph/9403052.
- Narayan, R., Yi, I., 1995a. Advection-dominated Accretion: Self-Similarity and Bipolar Outflows. *ApJ* 444, 231. doi:10.1086/175599, arXiv:astro-ph/9411058.
- Narayan, R., Yi, I., 1995b. Advection-dominated Accretion: Underfed Black Holes and Neutron Stars. *ApJ* 452, 710. doi:10.1086/176343, arXiv:astro-ph/9411059.
- Nomura, M., Ohsuga, K., Takahashi, H.R., Wada, K., Yoshida, T., 2016. Radiation hydrodynamic simulations of line-driven disk winds for ultra-fast outflows. *PASJ* 68, 16. doi:10.1093/pasj/psv124, arXiv:1511.08815.
- Novikov, I.D., Thorne, K.S., 1973. Astrophysics of black holes., in: *Black Holes (Les Astres Occlus)*, pp. 343–450.
- Ohsuga, K., Mori, M., Nakamoto, T., Mineshige, S., 2005. Supercritical Accretion Flows around Black Holes: Two-dimensional, Radiation Pressure-dominated Disks with Photon Trapping. *ApJ* 628, 368–381. doi:10.1086/430728, arXiv:astro-ph/0504168.
- Piran, T., 1978. The role of viscosity and cooling mechanisms in the stability of accretion disks. *ApJ* 221, 652–660. doi:10.1086/156069.

- Poutanen, J., Coppi, P.S., 1998. Unification of Spectral States of Accreting Black Holes. *Physica Scripta Volume T 77*, 57. [arXiv:astro-ph/9711316](#).
- Poutanen, J., Veledina, A., Zdziarski, A.A., 2018. Doughnut strikes sandwich: the geometry of hot medium in accreting black hole X-ray binaries. *A&A* 614, A79. doi:10.1051/0004-6361/201732345, [arXiv:1711.08509](#).
- Qian, L., Liu, B.F., Wu, X.B., 2007. Disk Evaporation-Fed Corona: Structure and Evaporation Features with Magnetic Field. *ApJ* 668, 1145–1153. doi:10.1086/521388, [arXiv:0707.0408](#).
- Qiao, E., Liu, B.F., 2009. Dependence of Spectral State Transition and Disk Truncation on Viscosity Parameter α . *PASJ* 61, 403. doi:10.1093/pasj/61.2.403, [arXiv:0901.0475](#).
- Qiao, E., Liu, B.F., 2012. The Emission from an Inner Disk and a Corona in the Low and Intermediate Spectral States of Black Hole X-Ray Binaries. *ApJ* 744, 145. doi:10.1088/0004-637X/744/2/145, [arXiv:1109.5824](#).
- Qiao, E., Liu, B.F., 2013. A Model for the Correlation of Hard X-Ray Index with Eddington Ratio in Black Hole X-Ray Binaries. *ApJ* 764, 2. doi:10.1088/0004-637X/764/1/2, [arXiv:1212.1770](#).
- Qiao, E., Liu, B.F., 2015. A disc corona-jet model for the radio/X-ray correlation in black hole X-ray binaries. *MNRAS* 448, 1099–1106. doi:10.1093/mnras/stv085, [arXiv:1501.03565](#).
- Qiao, E., Liu, B.F., 2017. The condensation of the corona for the correlation between the hard X-ray photon index Γ and the reflection scaling factor R in active galactic nuclei. *MNRAS* 467, 898–905. doi:10.1093/mnras/stx121, [arXiv:1701.04211](#).
- Qiao, E., Liu, B.F., 2018. A systematic study of the condensation of the corona and the application for $\Gamma_{2-10keV}$ - L_{bol}/L_{Edd} correlation in luminous active galactic nuclei. *MNRAS* 477, 210–218. doi:10.1093/mnras/sty652, [arXiv:1803.03375](#).

- Qiao, E., Liu, B.F., 2019. A model for the radio/X-ray correlation in three neutron star low-mass X-ray binaries 4U 1728-34, Aql X-1ad, and EXO 1745-248. *MNRAS* 487, 1626–1633. doi:10.1093/mnras/stz1365, arXiv:1905.05996.
- Qiao, E., Liu, B.F., 2020. A systematic study of the advection-dominated accretion flow for the origin of the X-ray emission in weakly magnetized low-level accreting neutron stars. *MNRAS* 492, 615–627. doi:10.1093/mnras/stz3510, arXiv:1912.05762.
- Qiao, E., Liu, B.F., Panessa, F., Liu, J.Y., 2013. The Disk Evaporation Model for the Spectral Features of Low-luminosity Active Galactic Nuclei. *ApJ* 777, 102. doi:10.1088/0004-637X/777/2/102, arXiv:1309.0090.
- Raymond, J.C., Cox, D.P., Smith, B.W., 1976. Radiative cooling of a low-density plasma. *ApJ* 204, 290–292. doi:10.1086/154170.
- Rees, M.J., Begelman, M.C., Blandford, R.D., Phinney, E.S., 1982. Ion-supported tori and the origin of radio jets. *Nature* 295, 17–21. doi:10.1038/295017a0.
- Reeves, J.N., Turner, M.J.L., Pounds, K.A., O’Brien, P.T., Boller, T., Ferrando, P., Kendziorra, E., Vercellone, S., 2001. XMM-Newton observation of an unusual iron line in the quasar Markarian 205. *A&A* 365, L134–L139. doi:10.1051/0004-6361:20000424, arXiv:astro-ph/0010490.
- Remillard, R.A., McClintock, J.E., 2006. X-Ray Properties of Black-Hole Binaries. *ARA&A* 44, 49–92. doi:10.1146/annurev.astro.44.051905.092532, arXiv:astro-ph/0606352.
- Różańska, A., Czerny, B., 2000. Two-phase radiative/conductive equilibrium in active galactic nuclei and galactic black holes. *MNRAS* 316, 473–478. doi:10.1046/j.1365-8711.2000.03429.x, arXiv:astro-ph/9906101.
- Różańska, A., Czerny, B., 2000. Vertical structure of the accreting two-temperature corona and the transition to an ADAF. *A&A* 360, 1170–1186. arXiv:astro-ph/0004158.

- Ruan, J.J., Anderson, S.F., Eracleous, M., Green, P.J., Haggard, D., MacLeod, C.L., Runnoe, J.C., Sobolewska, M.A., 2019. The Analogous Structure of Accretion Flows in Supermassive and Stellar Mass Black Holes: New Insights from Faded Changing-look Quasars. *ApJ* 883, 76. doi:10.3847/1538-4357/ab3c1a, arXiv:1903.02553.
- Sadowski, A., Narayan, R., 2016. Three-dimensional simulations of supercritical black hole accretion discs - luminosities, photon trapping and variability. *MNRAS* 456, 3929–3947. doi:10.1093/mnras/stv2941, arXiv:1509.03168.
- Shakura, N.I., Sunyaev, R.A., 1973. Reprint of 1973A&A....24..337S. Black holes in binary systems. Observational appearance. *A&A* 500, 33–51.
- Shapiro, S.L., Lightman, A.P., Eardley, D.M., 1976. A two-temperature accretion disk model for Cygnus X-1: structure and spectrum. *ApJ* 204, 187–199. doi:10.1086/154162.
- Shaviv, G., Wehrse, R., 1986. The vertical temperature stratification and corona formation of accretion disc atmospheres. *A&A* 159, L5–L7.
- Shi, F., Li, Z., Yuan, F., Zhu, B., 2021. An energetic hot wind from the low-luminosity active galactic nucleus M81*. *Nature Astronomy* 5, 928–935. doi:10.1038/s41550-021-01394-0, arXiv:2106.04041.
- Spitzer, L., 1962. *Physics of Fully Ionized Gases*.
- Spruit, H.C., Deufel, B., 2002. The transition from a cool disk to an ion supported flow. *A&A* 387, 918–930. doi:10.1051/0004-6361:20020294, arXiv:astro-ph/0108497.
- Stepney, S., 1983. Two-body relaxation in relativistic thermal plasmas. *MNRAS* 202, 467–481. doi:10.1093/mnras/202.2.467.
- Svensson, R., Zdziarski, A.A., 1994. Black hole accretion disks with coronae. *ApJ* 436, 599–606. doi:10.1086/174934.

- Taam, R.E., Liu, B.F., Meyer, F., Meyer-Hofmeister, E., 2008. On the Properties of Inner Cool Disks in the Hard State of Black Hole X-Ray Transient Systems. *ApJ* 688, 527–536. doi:10.1086/591901, arXiv:0807.3402.
- Taam, R.E., Liu, B.F., Yuan, W., Qiao, E., 2012. Disk Corona Interaction: Mechanism for the Disk Truncation and Spectrum Change in Low-luminosity Active Galactic Nuclei. *ApJ* 759, 65. doi:10.1088/0004-637X/759/1/65, arXiv:1209.4961.
- Taam, R.E., Qiao, E., Liu, B.F., Meyer-Hofmeister, E., 2018. A Model for Spectral States and Their Transition in Cyg X-1. *ApJ* 860, 166. doi:10.3847/1538-4357/aac50d, arXiv:1805.06076.
- Tanaka, Y., Shibazaki, N., 1996. X-ray Novae. *ARA&A* 34, 607–644. doi:10.1146/annurev.astro.34.1.607.
- Tombesi, F., Cappi, M., Reeves, J.N., Palumbo, G.G.C., Yaqoob, T., Braitto, V., Dadina, M., 2010. Evidence for ultra-fast outflows in radio-quiet AGNs. I. Detection and statistical incidence of Fe K-shell absorption lines. *A&A* 521, A57. doi:10.1051/0004-6361/200913440, arXiv:1006.2858.
- Walder, R., Melzani, M., Folini, D., Winisdoerffer, C., Favre, J.M., 2014. Simulation of Microquasars: The Challenge of Scales, in: Pogorelov, N.V., Audit, E., Zank, G.P. (Eds.), 8th International Conference of Numerical Modeling of Space Plasma Flows (ASTRONUM 2013), p. 141. arXiv:1405.0600.
- Wang, Q.D., Nowak, M.A., Markoff, S.B., Baganoff, F.K., Nayakshin, S., Yuan, F., Cuadra, J., Davis, J., Dexter, J., Fabian, A.C., Grosso, N., Haggard, D., Houck, J., Ji, L., Li, Z., Neilsen, J., Porquet, D., Ripple, F., Shcherbakov, R.V., 2013. Dissecting X-ray-Emitting Gas Around the Center of Our Galaxy. *Science* 341, 981–983. doi:10.1126/science.1240755, arXiv:1307.5845.
- Yang, X.H., Bu, D.F., Li, Q.X., 2018. Numerical Simulations of Winds Driven by Radiation Force from the Corona above a Thin Disk. *ApJ* 867, 100. doi:10.3847/1538-4357/aae4e2, arXiv:1809.09778.

- Yang, X.H., Bu, D.F., Li, Q.X., 2019. Magnetohydrodynamic Numerical Simulation of the Outflows Driven by Magnetic Field and Radiation Force from the Corona above a Thin Disk. *ApJ* 881, 34. doi:10.3847/1538-4357/ab2b47, arXiv:1906.07364.
- You, B., Tuo, Y., Li, C., Wang, W., Zhang, S.N., Zhang, S., Ge, M., Luo, C., Liu, B., Yuan, W., Dai, Z., Liu, J., Qiao, E., Jin, C., Liu, Z., Czerny, B., Wu, Q., Bu, Q., Cai, C., Cao, X., Chang, Z., Chen, G., Chen, L., Chen, T., Chen, Y., Chen, Y., Chen, Y., Cui, W., Cui, W., Deng, J., Dong, Y., Du, Y., Fu, M., Gao, G., Gao, H., Gao, M., Gu, Y., Guan, J., Guo, C., Han, D., Huang, Y., Huo, J., Jia, S., Jiang, L., Jiang, W., Jin, J., Jin, Y., Kong, L., Li, B., Li, C., Li, G., Li, M., Li, T., Li, W., Li, X., Li, X., Li, X., Li, Y., Li, Z., Liang, X., Liao, J., Liu, C., Liu, G., Liu, H., Liu, X., Liu, Y., Lu, B., Lu, F., Lu, X., Luo, Q., Luo, T., Ma, X., Meng, B., Nang, Y., Nie, J., Ou, G., Qu, J., Sai, N., Shang, R., Song, L., Song, X., Sun, L., Tan, Y., Tao, L., Wang, C., Wang, G., Wang, J., Wang, L., Wang, W., Wang, Y., Wen, X., Wu, B., Wu, B., Wu, M., Xiao, G., Xiao, S., Xiong, S., Xu, Y., Yang, J., Yang, S., Yang, Y., Yi, Q., Yin, Q., You, Y., Zhang, A., Zhang, C., Zhang, F., Zhang, H., Zhang, J., Zhang, T., Zhang, W., Zhang, W., Zhang, W., Zhang, Y., Zhang, Y., Zhang, Y., Zhang, Y., Zhang, Z., Zhang, Z., Zhao, H., Zhao, X., Zheng, S., Zhou, D., Zhou, J., Zhu, Y., Zhu, Y., 2021. Insight-HXMT observations of jet-like corona in a black hole X-ray binary MAXI J1820+070. *Nature Communications* 12, 1025. doi:10.1038/s41467-021-21169-5, arXiv:2102.07602.
- Yuan, F., Gan, Z., Narayan, R., Sadowski, A., Bu, D., Bai, X.N., 2015. Numerical Simulation of Hot Accretion Flows. III. Revisiting Wind Properties Using the Trajectory Approach. *ApJ* 804, 101. doi:10.1088/0004-637X/804/2/101, arXiv:1501.01197.
- Yuan, F., Narayan, R., 2014. Hot Accretion Flows Around Black Holes. *ARA&A* 52, 529–588. doi:10.1146/annurev-astro-082812-141003, arXiv:1401.0586.

- Yuan, W., Liu, B.F., Zhou, H., Wang, T.G., 2010. X-ray Observational Signature of a Black Hole Accretion Disk in an Active Galactic Nucleus RX J1633+4718. *ApJ* 723, 508–513. doi:10.1088/0004-637X/723/1/508, arXiv:1009.2808.
- Zdziarski, A.A., Gierliński, M., 2004. Radiative Processes, Spectral States and Variability of Black-Hole Binaries. *Progress of Theoretical Physics Supplement* 155, 99–119. doi:10.1143/PTPS.155.99, arXiv:astro-ph/0403683.
- Zdziarski, A.A., Lubiński, P., Smith, D.A., 1999. Correlation between Compton reflection and X-ray slope in Seyferts and X-ray binaries. *MNRAS* 303, L11–L15. doi:10.1046/j.1365-8711.1999.02343.x, arXiv:astro-ph/9812215.
- Zhu, Z., Stone, J.M., 2018. Global Evolution of an Accretion Disk with a Net Vertical Field: Coronal Accretion, Flux Transport, and Disk Winds. *ApJ* 857, 34. doi:10.3847/1538-4357/aaafc9, arXiv:1701.04627.